Applied Physics Express 7, 021701 (2014)
http://dx.doi.org/10.7567/APEX.7.021701

Optimization of alignment quality of ferroelectric liquid crystals by controlling anchoring energy

Qi Guo[1*], Abhishek K. Srivastava[1], Evgeny P. Pozhidaev[1,2], Vladimir G. Chigrinov[1], and Hoi-Sing Kwok[1]

[1]*Centre for Display Research, Hong Kong University of Science and Technology, Clear Water Bay, Kowloon, Hong Kong*
[2]*P.N. Lebedev Physical Institute of Russian Academy of Sciences, Moscow, Leninsky pr. 53, Russia*
E-mail: qguo@ust.hk

Received November 26, 2013; accepted January 3, 2014; published online January 23, 2014

Photoalignment allows precise control of anchoring energy, which enables the optimization of the alignment quality of ferroelectric liquid crystal (FLC) devices. Thus, the accurate measurement of the anchoring energy coefficient of the alignment layer in the FLC regime is critical. However, the methods proposed to date have several limitations and are not useful for FLC cells with a helical structure. In this paper, a method based on the evaluation of the optical relaxation time is proposed. The method is valid for both helical and helix-free FLC cells. The optimal anchoring energy to achieve the best alignment quality of FLCs is also investigated. © 2014 The Japan Society of Applied Physics

Modern liquid crystal (LC)-based electro-optical devices must have a fast electro-optical response, high contrast, wide viewing angle, and low power consumption.[1,2] Thus, ferroelectric liquid crystals (FLCs) attract an enormous amount of attention from researchers[3] for a variety of new applications.[4,5] The electrically suppressed helix (ESH) mode is one of the most promising electro-optical modes. Because it can provide a unique high alignment quality[5,6] and a small switching time of less than 100 μs[7,8] with a very weak electric field, the ESH mode is applicable to field sequential color (FSC) displays. Because color filters are not required for displaying primary colors in a temporal sequence, the efficiency and brightness of FSC liquid crystal displays (LCDs) are much higher than those of conventional LCDs.[9,10] The FSC LCD can be used to realize high-definition displays based on current semiconductor technologies. Another promising application of FLCs is their use in photonics devices, including fast shutters, special light modulators (SLMs), and gratings.[11,12] These devices can provide perfect electro-optical modulation up to the kHz frequency by the application of a very weak electric field.[13] Thus, FLCs are promising contenders for use in modern devices.[6–13] However, one of the prime objectives for the practical application of the FLC is to realize a high optical contrast with a low operating voltage. In this paper, a method of optimizing the alignment quality by adjusting the parameters of the photoalignment layer is proposed.

The anchoring energy of the alignment layer of an FLC is one of the most important parameters, because it affects both the optical quality of the FLC sample and its electro-optical modulation.[14,15] Evaluation of this parameter using experimental data provides a better understanding of the alignment processes for FLCs in different modes.[16,17] In addition, the reliable control of the anchoring energy of FLC cells facilitates further technological improvement of electro-optical devices.[18,19] General methods of performing anchoring energy measurements have been successfully explored for nematic LCs.[20] Moreover, considerable efforts have been directed toward developing a precise method for evaluating the anchoring energy of FLCs; Pozhidaev et al. have demonstrated a procedure of measuring the anchoring energy of the FLC based on a hysteretic FLC cell.[21] However, this procedure has several limitations such as no helical structure, no chevrons, and bistability. These limitations are difficult to meet in real cases.

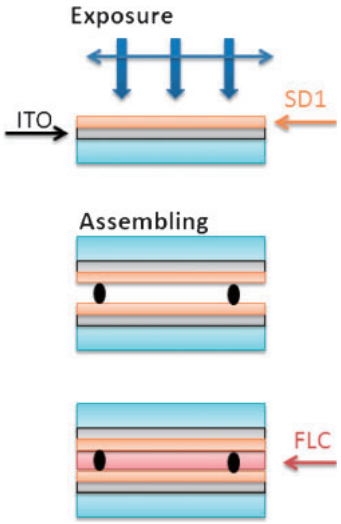

Fig. 1. Fabrication process and structure of FLC cell with photoalignment technique.

In this article, a method of measuring the anchoring energy by evaluating the relaxation time is proposed. The method is valid for both helical and helix-free structures. The results obtained using the proposed method are compared with published results[22] for the same photosensitive alignment material. The limitations of the proposed method are also discussed.

The fabrication process and geometry of the FLC cell are shown in Fig. 1. The FLC cell has been illuminated by normal incident light. The FLC layers are oriented in a homogenous configuration with the electric field being applied perpendicular to the helical axis of the chiral smectic C (SmC*) LC. The directors within the FLC helix are uniformly distributed in the helical cone because the cell thickness for the ESH mode is larger than the helix pitch and the helix is not suppressed by the substrate surface. When an electric field stronger than the helix unwinding field E_u is applied, it moves into the ESH regime, the helical cone disappears, and all the directors are arranged in the same direction according to the polarity of the electric field. Here, the helix unwinding field is given by $E_u = (\pi^2/16)(K_{22}q_0^2/P_S)$, where K_{22} is the elastic constant, P_S is the spontaneous polarization of the FLC, and q_0 represents the wave vector of the helix, given by $q_0 = 2\pi/p_0$, where P_0 is the helix pitch. Figure 2 shows the

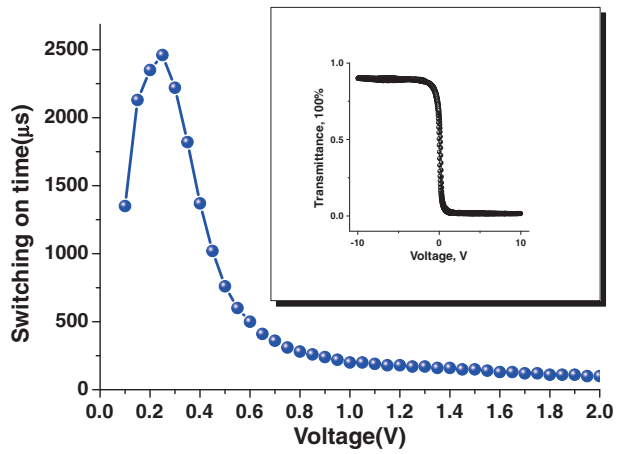

Fig. 2. Switching-on time vs driving voltage. Insertion: Hysteresis-free electro-optic switching of FLC cell at 0.001 Hz.

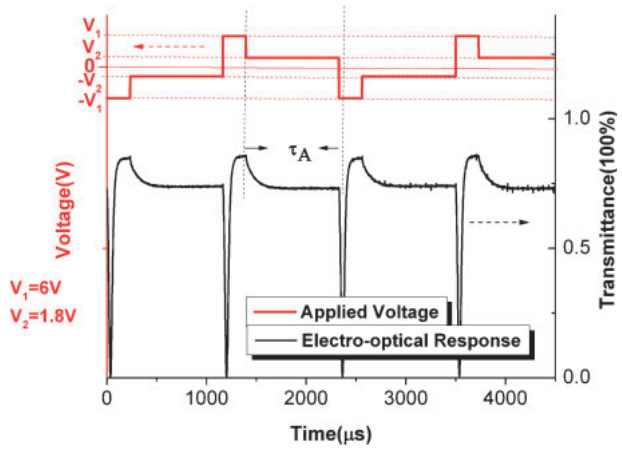

Fig. 3. Top: applied voltage to cell. Bottom: electro-optical response.

electric field dependence of the switching-ON time; the peak of the switching-ON time corresponds to the critical electric field. Moreover, as shown by the inset in Fig. 2, the ESH mode is characterized by a hysteresis-free electro-optical response, which indicates that the coercive force method cannot be used for measuring the anchoring energy coefficient in the ESH mode. Compared with the surface-stabilized (SS) FLC, it has a greater chance of eliminating defects and realizing high alignment quality because the alignment deals with the helix rather than the molecules. Furthermore, the EHS mode works when the helix is suppressed by the electric field; therefore, the scattering from the helix can also be eliminated.

The method of anchoring the energy coefficient measurement is performed in the regime where the elastic torque is suppressed by the spontaneous torque with an electric field stronger than the helix unwinding field. For FLC cells with a helical structure, the formation of the helix is a result of elastic torque. In the equilibrium state, without an external electric field, the total free energy could be minimized by balancing the elastic torque of the FLC material with the anchoring strength of the alignment layer. To obtain an accurate measurement of the anchoring energy coefficient using the relaxation process, the influence of the elastic torque should be excluded by applying a sufficiently strong electric field ($E > E_u$). Thus, to overcome the elastic torque, the electric pulse is applied and then the electric field is decreased to E_2 such that $E_2 \gg E_u$, as shown in Fig. 3. When the electric field is switched from a higher level E_1 to a lower level E_2, the molecular movement is driven only by the anchoring energy of the alignment layer. The FLC director $\varphi(z,t)$ distribution exhibits a quadratic decay from one equilibrium to another with the relaxation time:[23]

$$\tau_A = \gamma_\varphi d/4W_Q, \quad (\Delta W_P \ll W_Q). \tag{1}$$

In the experiment, we designed the test signal as shown in Fig. 3. The voltage amplitudes V_1 and V_2 were chosen to satisfy the requirement that $V_1 > V_2 \gg V_C$, where $V_C = d_{FLC}E_u$. Driven by the designed test signal, the electro-optical response of the FLC cell when the cell is placed between crossed polarizers with the helical axis parallel to polarizer $\beta = 0$ is shown at the bottom of Fig. 3. Another important issue is that the influence of anchoring from the alignment layers contains the dispersion part W_Q and the difference in the polar part ΔW_P if the configuration is asymmetric. Thus, we fabricated FLC samples oriented with a homogenous alignment using two symmetric substrates so that the difference in the polar anchoring strength between the two substrates is much smaller than the dispersion anchoring strength, i.e., $\Delta W_P \ll W_Q$.

The properties of the FLC mixtures used for the present investigation are given below.[24] FLC-595 has a spontaneous polarization of $P_S = 40\,\mathrm{nC{\cdot}cm^{-2}}$, a tilt angle of $\theta = 21.3°$, a rotational viscosity of $\gamma_\varphi = 0.022\,\mathrm{Pa{\cdot}s}$, an elastic constant of $K_{22} = 1.65 \times 10^{-11}\,N$, and a helix pitch of $P_0 = 0.72\,\mu\mathrm{m}$ at 22 °C. The phase transition sequence of FLC-595 is as follows: Cr → SmC* → SmA → Is at 22 °C, 38 °C, and 72 °C.

FD4004N has a spontaneous polarization value of $P_S = 61\,\mathrm{nC{\cdot}cm^{-2}}$, a tilt angle of $\theta = 22.5°$, and a helix pitch of $P_0 \approx 0.7\,\mu\mathrm{m}$ at 22 °C. The phase transition sequence of FD4004N is as follows: Cr → SmC* → SmA → N → Is at −19.2 °C, 70.7 °C, 98.6 °C, and 101.9 °C.

Two optically flat ITO-coated glass plates with small conducting areas were used as electrodes for preparing a sandwich-type sample holder. To analyze the anchoring energy strength, a photo-sensitive sulfonic dye (SD1) with different exposure doses was used as a photoalignment layer. The azodye material SD1 was provided by Dainippon Ink and Chemicals, and it was dissolved separately in dimethylformamide with a concentration of 0.4%. The photoalignment layer was prepared with normal exposure using a polarized UV lamp (Oriel 6925NS; 365 nm, $2\,\mathrm{mW\,cm^{-2}}$) for different exposure doses: 1.2, 3.6, 7.2, 18, 25.2, 36, 72, and $108\,\mathrm{J/cm^2}$. Testing cells with a cell gap of 1.5 μm and symmetrical boundary conditions for each alignment layer were prepared.

As shown at the bottom of Fig. 3, the electro-optical response waveform of the FLC sample under the designed testing signal exhibits a quadratic decay of the relaxation process. Exponential decay fitting is used to analyze the relaxation time, and the anchoring energy coefficient is calculated to be $W_Q = \gamma_\phi d/(4\tau_A)$. Figure 4 shows the measured anchoring energy coefficient of SD1 with different exposure doses. It demonstrates that the anchoring energy of the SD1 layer increases with a longer exposure time and tends to saturate. The anchoring energy coefficients are of the same order of magnitude as the coefficients measured using nematic liquid crystal cells.[25]

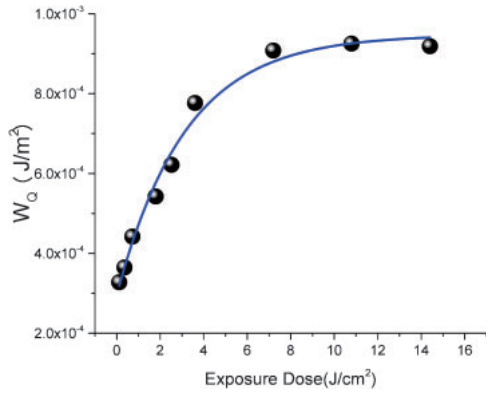

Fig. 4. Dependence of evaluated anchoring energy coefficient of SD1 layer on 1.5-μm-thick FLC-595 cell.

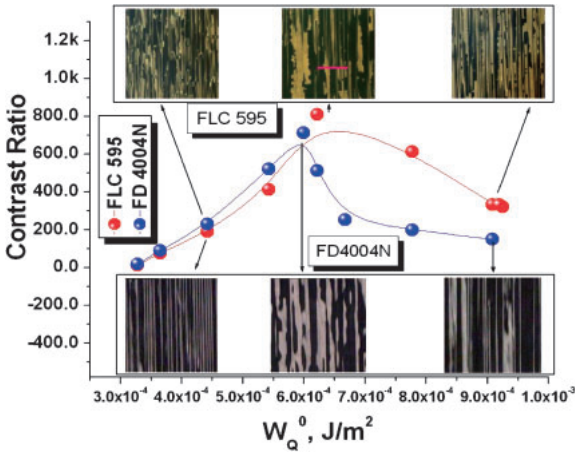

Fig. 5. Contrast ratio and texture of FLC cells with different anchoring energies of photoalignment layer. Textures are with size of the image is $150 \times 80\,\mu m^2$.

Figure 5 shows the dependence of the contrast ratio on the anchoring energy of the alignment layer. With a higher anchoring energy, the contrast ratio first increases to an optimal value and then tends to decrease. This explains the aligning mechanism of FLC cells with a helical structure. In the ESH mode, the elastic energy of FLC helix twisting is balanced by the normalized anchoring energy over the cell gap from the alignment layer; therefore, the external electric field can suppress the helix cone to achieve uniform bright and dark states corresponding to the two polarities of the applied electric field. With a lower anchoring energy, the alignment layer cannot provide sufficient strength to align the helix axis in one direction, whereas the alignment layer with a higher anchoring energy deforms the FLC helix. When the anchoring energy from the alignment layer is comparable to, but necessarily less than, the elastic energy of the FLC material, it exhibits a higher contrast ratio, as shown in Fig. 5. It was also observed that the optimal alignment quality corresponds to the equal areas of the two domains in the FLC cell texture. The two-domain structure is a result of the FLC arrangement corresponding to discrete distribution of the optical axis between the angles 0 and 2° and depending on the anchoring energy of the alignment layer and the FLC material parameters. The arrangement becomes uniform with an applied voltage higher than the critical voltage for helix unwinding. The anchoring strength shifting to either side of the optimal condition leads to the inequality of the two domain areas, and the contrast ratio decreases.

In conclusion, a method is proposed for measuring the anchoring energy of an FLC cell with a helix structure. This method is based on the analysis of the optical relaxation process in the ESH regime. The results obtained for the dispersion anchoring strength coefficient are compared with the values obtained using nematic liquid crystals. Although the proposed method has some limitations, as the FLC samples should be in the homogenous alignment, the difference in the polar anchoring strength between the two substrates should be much smaller than the dispersion anchoring strength, i.e., $\Delta W_P \ll W_Q$. Therefore, the proposed method can be used to measure the anchoring energy of FLC cells with and without a helix and is a powerful tool for evaluating the anchoring energy of the FLCs with pitch in the submicron region.

Acknowledgments This work is supported by the HKUST grants under CERG 614410, CERG 612409, and the partner's State Key Laboratory on Advanced Displays and Optoelectronics Technologies, Hong Kong university of science and technology, Hong Kong.

1) T. Takahashi, H. Furue, M. Shikada, N. Matsuda, T. Miyama, and S. Kobayashi, Jpn. J. Appl. Phys. **38**, L534 (1999).
2) J.-H. Lee, X. Zhu, and S.-T. Wu, J. Disp. Technol. **3**, 2 (2007).
3) I. Abdulhalim, Appl. Phys. Lett. **101**, 141903 (2012).
4) A. Kumar, J. Prakash, A. M. Biradar, and W. Haase, Appl. Phys. Express **3**, 091701 (2010).
5) A. K. Srivastava, W. Hu, V. G. Chigrinov, A. D. Kiselev, and Y.-Q. Lu, Appl. Phys. Lett. **101**, 031112 (2012).
6) E. P. Pozhidaev, M. Minchenko, V. Molkin, S. Torgova, V. G. Chigrinov, A. K. Srivastava, H. S. Kwok, V. Vashenko, and A. Krivoshey, Eurodisplay 2011, LCT-1.
7) L. Blinov, S. Palto, E. Pozhidaev, Y. Bobylev, V. Shoshin, A. Andreev, F. Podgornov, and W. Haase, Phys. Rev. E **71**, 051715 (2005).
8) E. P. Pozhidaev, V. G. Chigrinov, Y. P. Bobilev, V. M. Shoshin, A. A. Zhukov, A. L. Andreev, I. N. Kompanets, L. Xihua, E. E. Gukasjan, P. S. Komarov, O. A. Shadura, and H. S. Kwok, J. Soc. Inf. Disp. **14**, 633 (2006).
9) M. J. O'Callaghan, R. Ferguson, R. Vohra, W. Thurmes, A. W. Harant, C. S. Pecinovsky, Y. Zhang, S. Yang, M. O'Neill, and M. A. Handschy, J. Soc. Inf. Disp. **17**, 369 (2009).
10) X. J. Yu and H. S. Kwok, Appl. Phys. Lett. **89**, 031104 (2006).
11) A. D. Kiselev, E. P. Pozhidaev, V. G. Chigrinov, and H.-S. Kwok, Phys. Rev. E **83**, 031703 (2011).
12) J.-H. Na, J. Kim, Y. Choi, and S.-D. Lee, Appl. Phys. Express **6**, 054102 (2013).
13) Q. Guo, Z. Brodzeli, E. P. Pozhidaev, F. Fan, V. G. Chigrinov, H. S. Kwok, L. Silvestri, and F. Ladouceur, Opt. Lett. **37**, 2343 (2012).
14) E. Pozhidaev, V. Chigrinov, and X. Li, Jpn. J. Appl. Phys. **45**, 875 (2006).
15) L. A. Beresnev, V. G. Chigrinov, D. I. Dergachev, E. P. Poshidaev, J. Fünfschilling, and M. Schadt, Liq. Cryst. **5**, 1171 (1989).
16) A. Kiselev, V. Chigrinov, and E. Pozhidaev, Phys. Rev. E **75**, 061706 (2007).
17) M. I. Barnik, V. A. Baikaiov, V. G. Chigrinov, and E. P. Pozhidaev, Mol. Cryst. Liq. Cryst. **143**, 101 (1987).
18) F. Fan, A. K. Srivastava, V. G. Chigrinov, and H. S. Kwok, Appl. Phys. Lett. **100**, 111105 (2012).
19) W. Hu, A. Srivastava, F. Xu, J.-T. Sun, X.-W. Lin, H.-Q. Cui, V. Chigrinov, and Y.-Q. Lu, Opt. Express **20**, 5384 (2012).
20) V. Chigrinov, A. Muravski, H. S. Kwok, H. Takada, H. Akiyama, and H. Takatsu, Phys. Rev. E **68**, 061702 (2003).
21) E. P. Pozhidaev, V. G. Chigrinov, Y. P. Panarin, and V. P. Vorflusev, Mol. Mater. **2**, 225 (1993).
22) X. Li, V. M. Kozenkov, F. S. Yeung, P. Xu, V. G. Chigrinov, and H.-S. Kwok, Jpn. J. Appl. Phys. **45**, 203 (2006).
23) L. M. Blinov and V. G. Chigrinov, *Electrooptic Effects in Liquid Crystal Materials* (Springer, New York, 1994) Chap. 3.
24) Q. Guo, F. Fan, A. Murauski, L. Yao, and V. G. Chigrinov, Photonics Lett. Poland **3**, 26 (2011).
25) H.-S. Kwok, V. G. Chigrinov, H. Takada, and H. Takatsu, J. Disp. Technol. **1**, 41 (2005).